sustainable chemistry

MDPI

Article

Antimicrobial Activity of Gentamicin-Loaded Biocomposites Synthesized through Inverse Vulcanization from Soybean and Sunflower Oils

Ana S. Farioli [1], María V. Martinez [1,2], Cesar A. Barbero [2], Diego F. Acevedo [1,2] and Edith I. Yslas [3,*]

[1] Departamento de Tecnología Química, Facultad de Ingeniería, Research Institute for Energy Technologies and Advanced Materials (IITEMA), National University of Río Cuarto (UNRC)-National Council of Scientific and Technical Research (CONICET), Universidad Nacional de Río Cuarto, Río Cuarto X5800, Argentina; afarioli@exa.unrc.edu.ar (A.S.F.); mvmartinez@ing.unrc.edu.ar (M.V.M.); dacevedo@ing.unrc.edu.ar (D.F.A.)

[2] Departamento de Química, Facultad de Cs. Exactas Fisco-Química y Naturales, Research Institute for Energy Technologies and Advanced Materials (IITEMA), National University of Río Cuarto (UNRC)-National Council of Scientific and Technical Research (CONICET), Universidad Nacional de Río Cuarto, Río Cuarto X5800, Argentina; cbarbero@exa.unrc.edu.ar

[3] Departamento de Biología Molecular, Facultad de Cs. Exactas Fisco-Química y Naturales, Research Institute for Energy Technologies and Advanced Materials (IITEMA), National University of Río Cuarto (UNRC)-National Council of Scientific and Technical Research (CONICET), Universidad Nacional de Río Cuarto, Río Cuarto X5800, Argentina

* Correspondence: eyslas@exa.unrc.edu.ar

Abstract: Cross-linked polymers synthesized through inverse vulcanization of unsaturated vegetable oils (biopolymers) were used as matrices for incorporating gentamicin (GEN) to form a biocomposite that can amplify GEN antimicrobial activity against *Pseudomonas aeruginosa*. Two different biopolymers were synthesized using soybean (PSB) and sunflower (PSF) oils by inverse vulcanization cross-linked with sulfur in a 1:1 weight ratio. The study involves the synthesis and characterization of these biopolymers using FTIR and SEM as well as measurements of density and hydrophobicity. The results reveal the formation of biopolymers, wherein triglyceride molecules undergo cross-linking with sulfur chains through a reaction with the unsaturated groups present in the oil. Additionally, both polymers exhibit a porous structure and display hydrophobic behavior (contact angle higher than 120°). The biopolymers swell more in GEN solution (PSB 127.7% and PSF 174.4%) than in pure water (PSB 88.7% and PSF 109.1%), likely due to hydrophobic interactions. The kinetics of GEN sorption and release within the biopolymer matrices were investigated. The antibacterial efficacy of the resulting biocomposite was observed through the analysis of inhibition growth halos and the assessment of *P. aeruginosa* viability. A notable enhancement of the growth inhibition halo of GEN (13.1 ± 1.1 mm) compared to encapsulated GEN (PSF-GEN 21.1 ± 1.3 and PSB-GEN 21.45 ± 1.0 mm) is observed. Also, significant bactericidal activity is observed in PSF-GEN and PSB-GEN as a reduction in the number of colonies (CFU/mL), more than 2 $\log_{10}$ compared to control, PSF, and PSB, highlighting the potential of these biopolymers as effective carriers for gentamicin in combating bacterial infections.

Keywords: antibacterial; bacterial growth inhibition; biopolymers; biocomposites; inverse vulcanization

Citation: Farioli, A.S.; Martinez, M.V.; Barbero, C.A.; Acevedo, D.F.; Yslas, E.I. Antimicrobial Activity of Gentamicin-Loaded Biocomposites Synthesized through Inverse Vulcanization from Soybean and Sunflower Oils. *Sustain. Chem.* **2024**, *5*, 229–243. https://doi.org/10.3390/suschem5030015

Academic Editor: Dimitrios Giannakoudakis

Received: 12 June 2024
Revised: 11 July 2024
Accepted: 28 July 2024
Published: 1 August 2024

1. Introduction

Bacterial infections pose a significant global threat as they are fast spreading and claim millions of lives annually [1]. The emergence of multidrug-resistant bacteria intensifies the danger to human health, escalating medical expenses, protracting hospitalizations, and amplifying mortality rates. This critical issue has reached alarming proportions in recent times, profoundly impacting healthcare institutions, the environment, and patient well-being. The root causes lie in the inappropriate and indiscriminate use of antibiotics, coupled with

deficiencies in infection prevention and control [2,3]. Consequently, bacterial infections have become a prevalent and pressing challenge in contemporary healthcare. The microorganisms predominantly inhabiting intensive care units belong to the ESKAPE group, which includes *Enterococcus faecium*, *Staphylococcus aureus*, *Klebsiella pneumoniae*, *Acinetobacter baumannii*, *Pseudomonas aeruginosa*, and *Enterobacter* spp. Additionally, *Escherichia coli* stands out due to its widespread prevalence, marked by elevated resistance levels and persistent presence [4,5]. Recognizing the escalating global resistance to antimicrobial medicines, the World Health Organization (WHO) has published a list of antibiotic-resistant priority pathogens [6]. This list aims to stimulate research and development of new antibiotics, addressing the paramount threats to human health. Notably, *Pseudomonas aeruginosa* is identified as one of the most critical pathogens in this context [6]. The rising global issue of antibiotic resistance, with a particular focus on Gram-negative bacteria, underscores a critical challenge in pathogen control. *P. aeruginosa* is known for its Gram-negative aerobic nature and ability to move using polar flagella. It is considered an opportunistic pathogen, meaning it can cause infections in people with weakened immune systems or those who have undergone medical procedures. *P. aeruginosa* is implicated in a spectrum of infections affecting diverse anatomical sites such as the urinary tract, respiratory system, bones, joints, wounds, burns, and septicemia. Its impact is especially pronounced in individuals with both primary and acquired immunodeficiency, with a noteworthy prevalence observed among patients afflicted with cystic fibrosis [7]. *P. aeruginosa* exhibits distinctive characteristics facilitating its straightforward identification on agar, primarily owing to the production of water-soluble pigments. Notably, the bacterium synthesizes pyocyanin, manifesting as a blue-green pigment, and pyoverdine, presenting as a yellow-green pigment [8]. Beyond its detectability, *P. aeruginosa* is implicated in a diverse array of infections and employs various strategies to initiate and sustain infection, including multidrug resistance, biofilm formation, and antibiotic tolerance. Recognizing its critical status, the World Health Organization (WHO) designates *P. aeruginosa* as a "critical" pathogen [9], underscoring the imperative for urgent exploration and development of novel antibacterial agents specifically tailored to combat *P. aeruginosa* biofilms.

Gentamicin (GEN), an antibiotic belonging to the aminoglycoside family, has been widely employed for the treatment of diverse bacterial infections, including those affecting the urinary and respiratory tracts, blood, bones, and soft tissues [10]. These infections are primarily caused by Gram-negative bacteria, prominently including *P. aeruginosa* [9]. Aminoglycosides, as a significant antibiotic subgroup, demonstrate potent bactericidal effects against Pseudomonas infections. Gentamicin, specifically, acts by inhibiting bacterial protein synthesis. However, the efficacy of conventional antibiotic therapies in eliminating this pathogen is increasingly challenged due to its inherent and acquired resistance to such antibacterial agents. In response to this challenge, drug encapsulation in polymeric carriers has emerged as a promising strategy to enhance drug accumulation at the site of infection while minimizing associated toxicity [11,12]. This approach reflects a proactive effort to address the growing difficulty in combatting *P. aeruginosa* infections with conventional antibiotic treatments.

Various materials have been utilized for encapsulating active antibiotics, leading to an augmentation of their antibacterial properties. Among these are alginate, thermosensitive hydrogels, etc. [12–15]. This innovative approach addresses the increasing challenge of combating *P. aeruginosa* infections using conventional antibiotic treatments. On the other hand, in 2013, an innovative class of polymers with high sulfur content, termed "inverse vulcanized polymers", was introduced by Pyun and colleagues [16]. In contrast to traditional vulcanization, where sulfur is a minor component in the reaction feedstock, inverse vulcanization involves synthesizing polymers using elemental sulfur as major feedstock and a small number of vinylic comonomers. This process comprises ring-opening polymerization of elemental sulfur, followed by cross-linking with an unsaturated comonomer [17]. Various unsaturated comonomers have been employed in the synthesis of inverse vulcanized polymers [18]. Also, the inverse vulcanization reaction has been extended to produce

biopolymers from vegetable oils such as sunflower, soybean, and palm oil [17,19,20]. These materials have been suggested for diverse applications crossing areas such as purifying water contaminated with mercury [19,21], decontaminating water tainted with hydrocarbons [17], and facilitating the controlled release of NPK fertilizers and antibacterial surfaces [22,23].

In the same direction, different petroleum-based monomers have been used to generate copolymers by inverse vulcanization and tested as antibacterial materials. Dop et al. conducted an investigation into the impact of high sulfur polymers, synthesized with various petroleum-based divinyl comonomers and at varying sulfur/comonomer ratios, on the antibacterial properties of materials [24]. Concurrently, in separate studies, they documented the formulation of petroleum-based polymeric nanoparticles with elevated sulfur content, which exhibited notable inhibitory effects against significant bacterial pathogens such as Gram-positive methicillin-resistant *Staphylococcus aureus* and Gram-negative *Pseudomonas aeruginosa*. The authors postulated that this observed effect may arise from the interaction between the polymeric nanoparticles and cellular thiols, potentially serving as a mechanism of action against bacterial cells. This hypothesis finds support in their experimental findings, which demonstrate a discernible reaction with cysteine, a representative thiol compound [25]. Furthermore, other researchers undertook a comparative analysis of the antibacterial efficacy of two distinct petroleum-based inverse vulcanized sulfur polymers: sulfur-co-diisopropenyl benzene (S-DIB) and sulfur dicyclopentadiene (S-DCPD) [26]. In contrast, our investigation presents novel insights into the practical application of two biopolymers synthesized through reverse vulcanization, employing vegetable oils as monomers, making full biobased materials without any petroleum-based monomer. Furthermore, our research involves the utilization of polymers derived from sunflower and soybean vegetable oils, which at the moment have not been previously published or examined for their antibacterial properties. Also, it demonstrates that these biopolymers present an ability to adsorb and release gentamicin, making these materials novel biocomposites. Moreover, the liberation of gentamicin produces an antibacterial effect higher than gentamicin in solution. Despite their versatility and sustainability, there is a notable lack of studies exploring the use of these materials for encapsulating antibiotics, aiming to enhance the efficacy to combat pathogenic bacteria while simultaneously minimizing the number of antibiotics required.

In summary, this research demonstrates an extension of the application of such materials, the effective application of two biopolymers synthesized through inverse vulcanization using monomer vegetable oils as matrices capable not only of incorporating gentamicin but also of producing antimicrobial activity against *P. aeruginosa*. Additionally, the research studies the kinetics of gentamicin sorption to form an antimicrobial biocomposite. Also, the GEN release within these biopolymer matrices is analyzed. Finally, the antibacterial efficacy of this nanocomposite is assessed through the analysis of the inhibition growth halo and the bacterial viability of *P. aeruginosa*.

Largely, this study contributes valuable insights into the application of biopolymers derived from soybean and sunflower oils for drug delivery, showcasing their proficiency in generating antimicrobial activity against *P. aeruginosa*. The presented biocomposite holds promise for future advancements in the development of innovative and efficient drug delivery systems using full biobased polymers.

2. Materials and Methods

Materials. Elemental sulfur (S_8) used as monomer was obtained from Aldrich (purity > 99%). Commercial sunflower oil Natura®, from AGD (General Deheza, Cordoba, Argentina) (SF) and degummed soybean oil donated by Mol-Prot S.A., Moldes, Córdoba, Argentina (SF) were employed without further purifications. Commercial gentamicin sulfate (GEN) (80 mg/mL) was purchased from Laboratorios Richet (Tres Arroyos, Buenos Aires, Argentina). Phosphate buffer solution (PBS) at pH 7 was prepared using sodium chloride (2.13 mM NaCl), potassium chloride (2.68 mM KCl), dibasic sodium

phosphate (10 mM Na_2HPO_4), and monobasic potassium phosphate (1.76 mM KH_2PO_4). Water used in this work was bi-distilled.

Biopolymers synthesis and characterization. The biopolymer synthesis was carried out by the inverse vulcanization method, as described in our previous work [17]. Briefly, elemental sulfur and vegetable oil (in a 1:1 weight ratio) were heated at 160 °C in separate beakers. Once the desired temperature was reached, both reagents were mixed and kept under heating (up to 180 °C) and stirring (900 rpm). After 15–20 min, the viscosity of the reaction mixture significantly increased, at which point the stirring was stopped and the reaction mixture was removed from the heater. The product was allowed to cool at room temperature. The biopolymer obtained from sunflower oil is designated as PSF, and with soybean oil is designated as PSB.

The synthesized biopolymers (PSF and PSB) and the vegetal oils sunflower (SF) and soybean oils (SB) were characterized in a previous study [17]; the obtained properties of these biopolymers are shown in Table 1:

Table 1. Physicochemical characterization of the biopolymers and vegetable oils [17].

Biopolymer	**Density [g/mL]**	**% Free Sulphur**	**Contact Angle [°]**
PSF	0.49 ± 0.09	34.63 ± 8	121.20 ± 0.80
PSB	0.70 ± 0.06	18.50 ± 9	139.00 ± 1.00
Vegetal oil	Iodine index		
SF	115		
SB	126		

Also, in order to ensure the effectivity of the synthesis, the biopolymers (PSF and PSB) and the vegetal oils, sunflower (SF) and soybean (SB), were characterized using FTIR-ATR spectroscopy in absorbance mode (Bruker Tensor 27 spectrometer using a ZnSe single-reflection attenuated total reflectance). Duplicate spectra per sample were obtained with 20 scans per spectrum at a spectral resolution of 4 cm^{-1} in the wavenumber range from 4000 to 500 cm^{-1}. As a reference, the background spectrum of air was collected before the acquisition of each sample spectrum.

The morphology of the polymers was studied using scanning electron microscopy (SEM). Firstly, the biomaterials (1 × 1 × 0.3 cm) were freeze-dried using a RIFICOR L-T4 freeze dryer (at −60 °C, under dynamic vacuum, for 48 h). Second, the samples were sputter-coated with a thin layer of gold for 90 s at a current of 40 mA and a pressure of 0.4 mbar under an argon atmosphere. The polymer morphology was examined through scanning electron microscopy (Carl Zeiss–Sigma, 0.1–30 kV accelerating tension). A voltage of 3 kV was applied for capturing scanning electron microscopy (SEM) images of the samples.

An important property of these materials is their hydrophilic/hydrophobic nature and their capacity to incorporate aqueous solutions. To investigate this property, static contact angle measurements were performed using the optical tensiometer Theta Flow (Biolin Scientific). A bi-distilled water drop (5 µL) was deposited on the biopolymer surface, and the contact angle was recorded at the initial time (t = 0 s) and after 5 min for a total of 25 min. The contact angle analysis was conducted using the OneAttension® software, and the reported values represent the average of five photographs.

Moreover, to determine the materials' capacity to incorporate water and GEN/PBS buffer, the swelling (Sw) and percentage (%Sw) were measured as follows: the dried materials were first weighed and then placed in the solution at room temperature. At specific time intervals, the biopolymers were removed from the solution, superficially dried

with tissue paper, and re-weighed using an analytical balance. The Sw was calculated as a function of time according to the Equation (1):

$$Sw(t) = \frac{w(t) - ws}{ws} \quad (1)$$

where w(t) represents the weight of the wet biopolymers at a given time, and ws is the weight of the dry biopolymer. Also, the swelling percentage can be calculated using Equation (2):

$$\%Sw(t) = Sw(t) \cdot 100 \quad (2)$$

Graphs of %Sw vs. time were used to analyze the swelling kinetics. Moreover, the swelling percentage in equilibrium ($\%Sw_{eq}$) was calculated when the biopolymer's weight no longer changed with time (w_{eq}).

Biocomposites preparation: PSF and PSB load with GEN. To measure the amount of gentamicin sorbed and released by each biopolymer PSF and PSB, the UV–visible absorption band of GEN at 255 nm was followed using a Hewlett Packard 8453 spectrophotometer. Previously, a calibration curve of the GEN/PBS obtained an absorptivity coefficient of 2.93 mL/(mg·cm).

Gentamicin sorption. Sorption kinetics were carried out at room temperature. A biopolymer piece was weighed (m_{Bp}) (ca. 0.04 g) and placed into 4 mL of GEN/PBS solution at 0.5 mg/mL. The biopolymer weight and the UV–visible spectra of the external solution were measured at regular intervals of time and the absorbance at 255 nm was obtained. Sorption capacities (q), the mg_{GEN} loaded per gram of biocomposite (Bc) were calculated using Equation (3):

$$q(t) = \left[\frac{mg_{GEN}}{g_{Bc}}\right] = \frac{Co \cdot Vo - \left[C(t) \cdot \left(Vo - \left(\left(m(t) - m_{Bp}\right)/\rho\right)\right]\right.}{m_{Bp}} \quad (3)$$

in which m(t) is the mass of the Bc at time t, C(t) represents the concentration of GEN in external solution at time t, while m_{Bp} and Co denote the initial mass of the biocomposite and the initial concentration of GEN. Vo represents the initial volume of the GEN/PBS solution and ρ is the water density at 25 °C.

Gentamicin release. The release of GEN from each biocomposite was measured. For this purpose, a dried polymer piece was weighed (0.032 g) and then placed in 2 mL of GEN/PBS solution at 5 mg_{GEN}/mL for one hour at ambient temperature. Subsequently, the pre-loaded biocomposite was transferred to 4 mL of PBS buffer (pH 7), UV–visible spectra of the external solution were recorded. The GEN external concentration was calculated using a calibration curve of the GEN/PBS at 255 nm, previously determined, obtaining an absorptivity coefficient of 2.93 $mL \cdot mg^{-1} \cdot cm^{-1}$. Also, the released GEN milligram per gram of biocomposite (L^G) vs. time was obtained to study the GEN release kinetic, Equation (4). It is important to clarify that the 5 mg/mL concentration of GEN was used solely in this experiment. This specific concentration was chosen to measure the gentamicin released, due to the low sorption properties of the biopolymers and the low absorptivity of gentamicin.

$$L^G = \frac{C_{GEN}(t) \cdot V_d}{m_{Bc}} \quad (4)$$

where the C_{GEN} is the concentration of GEN obtained at different time, V_d is the external volume (4 mL), and m_{Bc} is the dry mass of the biocomposite.

Biological Assay

Storage and Bacteria preparation. *Pseudomonas aeruginosa* (strain PAO1) was preserved for long-term storage in Glycerol at −80°. When required for experimental use, glycerol stocks were thawed and plated on LB agar. The inoculum was prepared by swabbing one colony into 10 mL of LB broth within an Erlenmeyer of 50 mL. This inoculum was then left

to incubate overnight at 150 rpm and 37 °C. Subsequently, the culture was initiated using 100 µL from inoculum, which was introduced into 10 mL of fresh LB broth. This culture was cultivated for approximately 4 h under conditions of constant agitation at 150 rpm and a temperature of 37 °C, reaching the desired exponential growth phase [27].

Growth inhibition halo. The antibiotic susceptibility of PAO1 was evaluated using a disc diffusion method. For antimicrobial susceptibility testing, 6 mm diameter filter paper discs were sterilized and loaded with 5 µL of antibiotic solution (0.5 mg/mL). These discs were then placed on *P. aeruginosa* lawns, and the plates were incubated at 37 °C for 24 h to measure gentamicin inhibition halos. Biopolymers (0.032 g PSF and 0.031 g PSB) previously sterilized by 20 min UV radiation per side, and the biocomposites obtained loading both Bp during 45 min in a GEN solution 0.5 mg/mL, were placed on *P. aeruginosa* lawns and incubated in parallel with the paper disc in the same condition. The plates were subsequently examined for the presence or absence of inhibition halos around the tested samples, and the diameter of the inhibition halos was informed. Gentamicin-impregnated filter paper served as the positive control for all experiments. Each test sample was assessed in triplicate across four independent experiments [27].

Antibacterial activity: colony-forming count method. The antibacterial activity of the samples (previously sterilized by 20 min UV radiation per side) was assessed against Gram-negative *P. aeruginosa* by plate-counting method. The experiment was realized in an exponential phase covered with 1 mL saline solution containing approximately 10^6 colony-forming units per milliliter (CFU/mL) concentration of *P. aeruginosa*.

This test was carried out in triplicate, employing four independent experiments: (i) Control: 4 microliters of GEN (0.5 µg/mL), 2 µg GEN; (ii) Biopolymers: PSF (0.032 g) and PSB (0.032 g); (iii) Biocomposites: (PSF-GEN and PSB-GEN) obtained loaded PSF (0.032 g) and PSB (0.032 g) with gentamicin 4 mL 0.5 mg/mL during 45 min, taking into account the global coefficient of release at the equilibrium; the Bc PSF-GEN release 2.3 µg GEN and PSB 1.9 µg.

Then, the GEN, biopolymers (PSF and PSB), and the biocomposites PSF-GEN and PSB-GEN were added in 1 mL of physiological solution containing a 10^6 CFU.

After that, the suspension (1 mL 10^6 CFU/mL) with GEN, both Bp and both Bc were incubated for 24 h in a shaking incubator at 37 °C. The samples were vigorously vortexed for 5 min to remove all the bacteria (adhered and not adhered). Then, 100 µL of suspension was taken and serially diluted with saline solution. Subsequently, 20 µL of diluted bacteria solution with 0.8% NaCl was spread on the LB agar plates in triplicate and incubated at 37 °C for 24 h. After a 24 h culture at 37 °C, colonies formed on the agar plates were counted.

Statistical Analysis. All experiments were done in triplicates in three independent experiments and the results were reported as averages ± standard deviation or standard error. All data were analyzed by applying the Origin® software, by a one-way ANOVA test followed by post hoc statistical test using the Tukey test. Differences were considered statistically significant at * $p < 0.01$.

3. Results and Discussion

Physicochemical properties of biomaterials. Sunflower oil (SB) and soybean oil (SF) were analyzed by Fourier-transform infrared spectroscopy with attenuated total reflectance (FTIR-ATR) to assess their physicochemical properties. Two peaks were observed in the spectra (Figure 1A, top): one at 3008 cm^{-1} corresponding to stretching vibrations of the vinylic hydrogen in fatty acids, and another at 1700 cm^{-1} indicative of carbonyl (C=O) groups present in the triglyceride backbone. These characteristic signals confirm the presence of fatty acids in the vegetable oils [17].

During the synthesis, thiyl sulfur radicals are generated at temperatures above 160 °C and react with the double bonds, allowing cross-linking [28]. Figure 1A (FTIR spectra for both biopolymers) reveals the disappearance of the unsaturated H-C=C signal at 3008 cm^{-1}, previously observed in the vegetable oils. This previously observed peak in the vegetable oils confirms the successful addition of the thiyl radical to the double bonds

during biopolymer formation, creating the cross-linked network. Interestingly, soybean oil possesses a higher iodine value (126) compared to sunflower oil (115), implying a greater degree of unsaturation in its fatty acid chains. Consequently, PSB, derived from soybean oil, is expected to exhibit a higher cross-linking density compared to PSF, due to the availability of more reactive double bonds for participation in the cross-linking process [17,29].

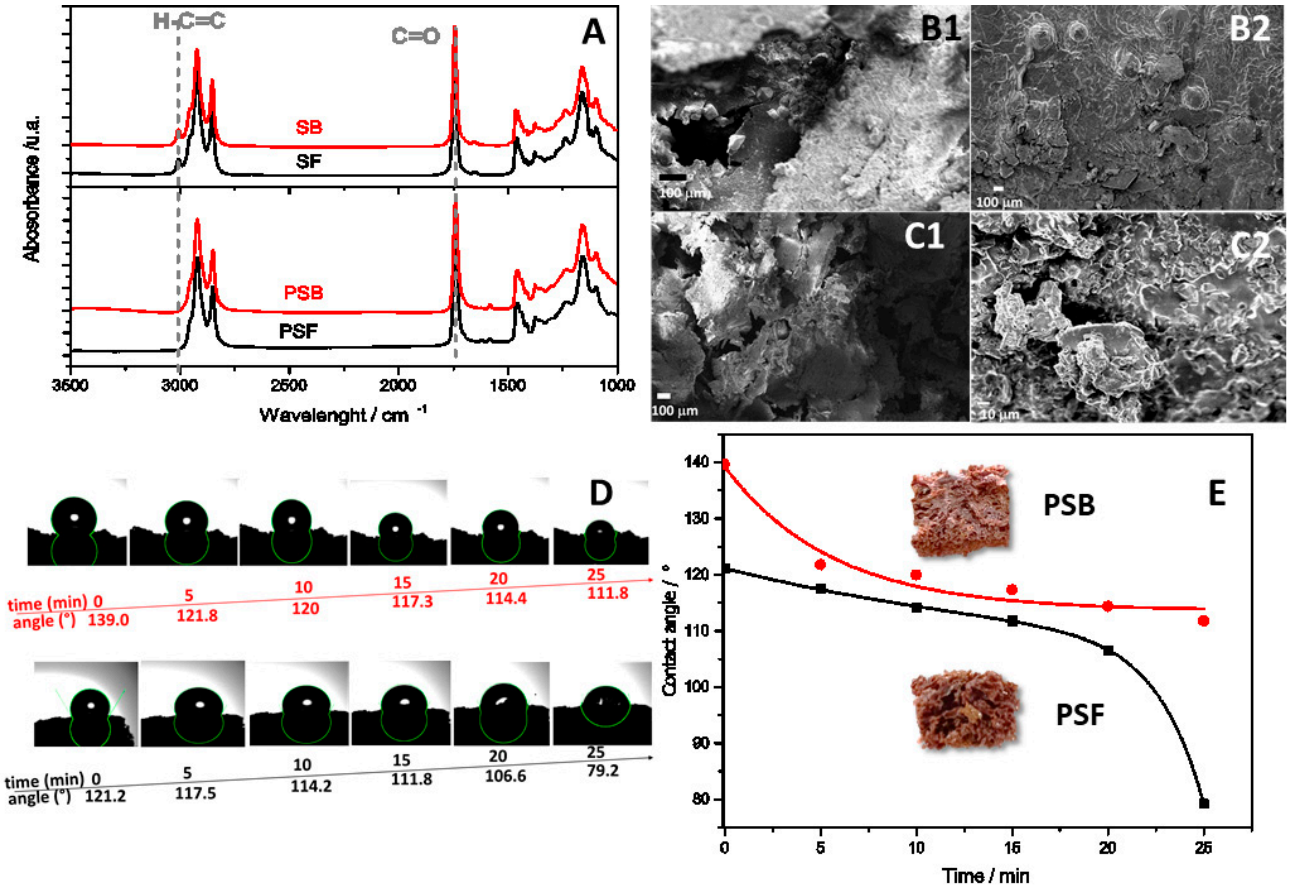

Figure 1. Characterization of biopolymers: (**A**) FTIR-ATR spectra of vegetable oils (top) SB (red) and SF (black) and biopolymers (down) PSB (red) and PSF (black). (**B1**,**B2**) SEM images of PSB. (**C1**,**C2**) SEM images of PSF. (**D**,**E**) Contact angle vs. time of PSB (red) and PSF (black).

Electron Microscopy (SEM) images are presented in Figure 1B and reveal that the porous structure is more compact in the case of PSB than in PSF (Figure 1C). This hypothesis finds support in the density measurements, with PSB exhibiting the highest density (0.70 g/mL $\pm$ 0.06) in comparison to PSF (0.49 g/mL $\pm$ 0.09). Also, optical photographs presented in Figure 1E reveal an irregular and porous structure resembling that its structure is similar to a sponge, wherein distinct macro-pores are prominently discernible [17].

Hydrophilic/hydrophobic property and wettability. The contact angle between the biomaterial surface and a water droplet was measured over a 25 min period, as depicted in Figure 1D,E. At the initial time (t = 0), the contact angle for both materials, PSF and PSB, exceeded 90°, indicating their hydrophobic nature. Additionally, it is observed that the contact angle decreases over time, with a more pronounced reduction for PSF compared to PSB, reaching 79.2° and 111.8° at 25 min, respectively. This outcome is attributed to their irregular morphological features and the presence of micro- and macro-porosity, along with the lower cross-linking of the soybean oil polymer. Despite the hydrophobic nature of the materials, once water wets the pores, wettability is facilitated, enabling the sorption of aqueous solutions [30]. As depicted in Figure 1E, the contact angle of PSF gradually decreases during the initial 20 min and subsequently experiences a sudden decrease between the final 20 and 25 min. In contrast, the contact angle of PSB decreases

by 20 degrees within the first 5 min and then remains relatively constant. This observed behavior may be attributed to the inherent structure and cross-linking of the biopolymers. In the case of PSB, the higher degree of cross-linking facilitates rapid wetting of the smallest pores within the initial 5 min, after which they fill gradually without significant changes in the contact angle. Conversely, PSF, characterized by larger pores, exhibits a slower wetting process during the first 20 min, followed by a rapid filling in the last 5 min. These findings align perfectly with the structural observations made using optical and electron microscopy, as well as the cross-linking degree determined by analyzing the amount of free sulfur.

Biopolymers swelling kinetics. The swelling kinetics was carried out in water and the GEN solution, as shown in Figure 2A,B respectively. In the analysis of the swelling capacity of a material, two parameters must be considered: the equilibrium swelling capacity (%Sw_{eq}) and the initial sorption rate (ks). When a biopolymer in its initial state comes into contact with solvent molecules, the solvent interacts with the Bp surface and permeates the polymeric network [31]. Normally, the network begins to swell, facilitating the incorporation of additional solvent molecules into the material network. The equilibrium swelling capacity and the initial adsorption rate depend on the degree of cross-linking and to the hydrophilic/hydrophobic character of the material [27]. The process can be evaluated through pseudo-first-order using the Equation (5) [32–35].

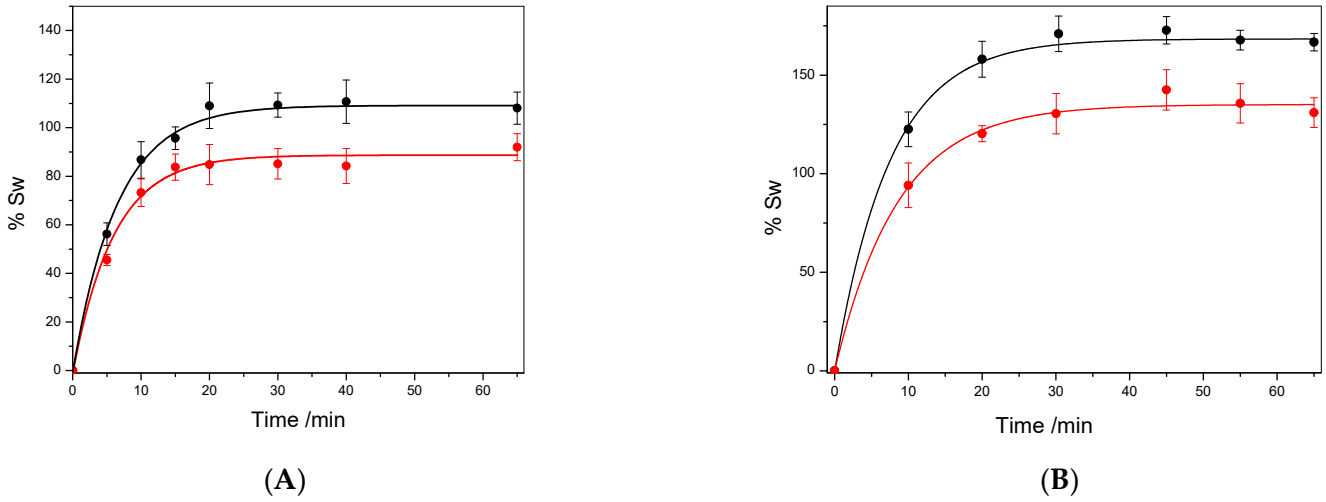

Figure 2. Swelling kinetics for PSF (black) and PSB (red), dots represent the experimental data and lines represent the first-order kinetic fitting for (**A**) water and (**B**) 0.5 mg/mL PBS/GEN solution.

$$\frac{d\%Sw}{dt} = k_s \cdot \left(\%Sw_{eq} - \%Sw\right) \quad (5)$$

where $\frac{d\%Sw}{dt}$ is swelling ratio, ks (1/min) is the rate constant of swelling, and %Sw_{eq} denotes the maximum degree of swelling at equilibrium. After definite integration by applying the initial conditions, %Sw = 0 at t = 0 and, %Sw = %Sw, at t = t, Equation (5) becomes in Equation (6).

$$\%Sw = \%S_{weq} \cdot \left(1 - e^{-ks \cdot t}\right) \quad (6)$$

Figure 2A,B, shows the curve %Sw vs. *t*, fitting using Equation (6), and the values ks and %Sw_{eq} (the rate constant of first-order sorption and the equilibrium swelling) are shown in Table 2.

Table 2. Parameters obtained from the first fitting of the swelling kinetic data.

	Pseudo-First-Order Fitting		Nature of Water Diffusion ± SE
	Sw_{eq}	ks	*n*
PSB in W	88.7 ± 2.4	0.161 ± 0.021	0.466 ± 0.096
PSF in W	109.1 ± 3.9	0.153 ± 0.024	0.470 ± 0.059
PSB in PBS/GEN	127.7 ± 5.9	0.085 ± 0.005	0.275 ± 0.028
PSF in PBS/GEN	174.1 ± 8.9	0.105 ± 0.012	0.306 ± 0.048

Moreover, a simple and useful empirical equation is commonly used to determine the mechanism of diffusion in polymeric networks (Equation (7)) [31].

$$\frac{Sw(t)}{Sw_{eq}} = k_c \cdot t^n \quad (7)$$

The parameter *n* obtained fitting graphics Sw vs. time is depicted in Table 2.

As can be seen in Figure 2, the swelling kinetics of both polymers in the PBS/GEN solution exhibit a similar profile to that in water. Moreover, notably, the equilibrium swelling values in the PBS/GEN solution are more elevated for both materials than in water. This phenomenon can be attributed to GEN's affinity for biopolymers, as GEN presents a more hydrophobic character than pure water, resulting in a stronger interaction with the hydrophobic biopolymer matrix. Moreover, as can be observed in Table 1, the model indicates that PSF not only exhibits a higher equilibrium swelling capacity in water and PBS/GEN compared to PSB but also almost the same initial sorption rate (ks). These findings align with a structure characterized by lower cross-linking and lower density, allowing a higher quantity of solvent in the matrix, in contrast to PSB (see Table 2). The kinetics further demonstrates that 45 min is sufficient for reaching equilibrium swelling in the PBS/GEN solution. Furthermore, the swelling exponent (n) has been probed as a crucial parameter in examining the diffusion characteristics, providing insights into the transport mechanism or type of diffusion [31]. When *n* values are less than 0.50, Fickian diffusion is suggested, whereas values between 0.5 and 1 indicate non-Fickian diffusion. In our study, the observed *n* values ranging from 0.275 to 0.470 consistently indicate Fickian diffusion across all the studied cases [32].

Gentamicin Sorption and Liberation

Sorption kinetics for the biocomposites in the PBS/GEN solution is illustrated in Figure 3A. The gentamicin sorption capacities (q, mg_{GEN}/g_{Bc}) were determined using Equation (3). The kinetics data were obtained by fitting the experimental data to the exponential model, as outlined in Equation (8).

$$q(t) = q^G_{eq}\left(1 - e^{-k_G \cdot t}\right) \quad (8)$$

where $q^G{}_{eq}$ represents the gentamicin sorption capacity in equilibrium, k_G is the initial sorption rate, and t is the time.

Furthermore, the maximum sorption capacity is attained at approximately 45 min for both biocomposites, leading to equilibrium conditions. The maximum q^G that could be achieved is 1.5 $mgGEN/g_{Bp}$ for PSF and 0.52 $mgGEN/g_{Bp}$ for PSB. Taking into account that the biopolymer mass used in the experiment was 0.04 g, and that the total mass of GEN present in the sorption solution was 2 mg (4 mL of 0.5 mg_{GEN}/mL), it is possible to calculate the efficiency of sorption (η) at the equilibrium using the Equation (9) [36].

$$\eta_s = \frac{\text{mass of GEN in the Bc}}{\text{mass of GEN in the solution}} \cdot 100 \quad (9)$$

Using Equation (9), the efficiency sorption reached is 3% for PSF and 1% for PSB, respectively. The value indicates that 0.04 g of the PSF loads 0.06 mgGEN, after 45 min of sorption in 4 mL of 0.5 mg/mL. In the same direction, PSB can load 0.02 mgGEN in the same conditions. The higher q^G value for PSF is in agreement with the swelling, which depends mainly on its lower cross-linking and lower density.

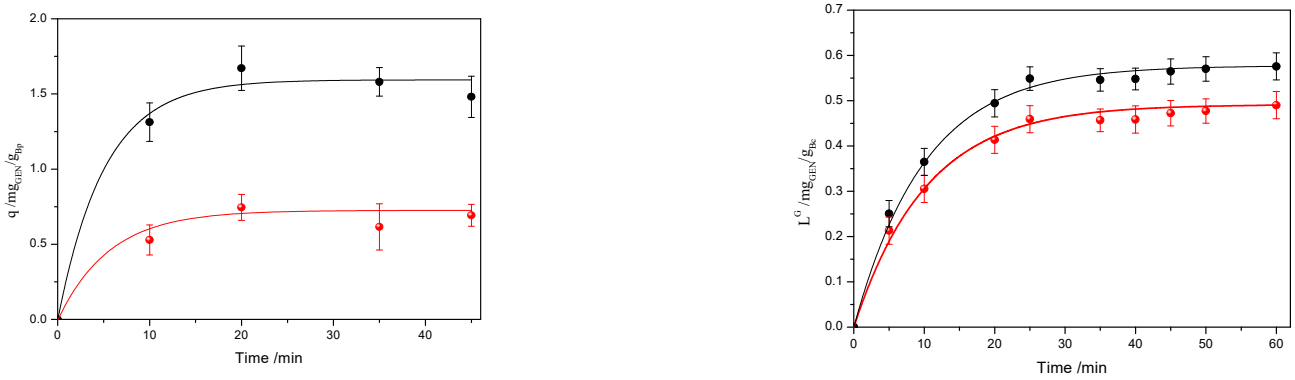

(**A**) (**B**)

Figure 3. Kinetics for PSF (black) and PSB (red), dots represent the experimental data: (**A**) sorption of 0.5 mg/mL PBS/GEN solution, (**B**) Liberation from biocomposites loaded with 5 mg_{GEN}/mL in PBS solution. Line represents the exponential fitting of the experimental data.

Figure 3B shows the GEN liberation profile of both biocomposites; as can be seen, the release of this molecule exhibits a similar pattern. Also, in both cases, the maximum quantity of GEN is released in less than one hour. Moreover, observing Figure 3B, the maximum values of L^G are 0.57 for PSF-GEN and 0.49 for PSB-GEN. At time 35 min, the PSF reaches a higher value and also has a higher speed of release than PSB. This fact is probably due to the more open structure because it is a less cross-linked polymer that allows easy diffusion of the loaded compound than in PSB.

It is important to note that the PSB-GEN biocomposite, despite a low sorption of 67% less than PSF-GEN, shows a GEN release of only 14% less than PSB. This result clearly indicates that the biocomposite PSF-GEN presents more affinity for the GEN than PSB, probably due to the chemical interaction between the GEN and the biopolymer.

Based on Figure 3B, it is possible to obtain a global coefficient of release at the equilibrium (ηL) as the ratio between the mg of GEN released with respect to the mg GEN in the solution of sorption. The ηL for PSF-GEN gives a value of 1.15×10^{-3} and for PSG-GEN 9.8×10^{-4}.

Antibacterial activity: Formation of inhibition growth halo. *Pseudomonas aeruginosa*, an opportunistic pathogen, is known to cause various acute and chronic infections in immunocompromised patients. In this study, we investigated the antimicrobial properties of biopolymers synthesized using sulfur, a by-product of industries, and vegetable oils derived from sunflower or soybean. These biopolymers were synthesized through inverse vulcanization. It is important to note that for antimicrobial susceptibility testing, 6 mm diameter filter paper discs were loaded with 5 µL of antibiotic solution (0.5 mg/mL), containing at the moment of the test 2.5 µgGEN. Additionally, we explored the antimicrobial effects of biocomposites (Bc) loaded with gentamicin (PSF-GEN and PSB-GEN). The Bc were obtained by loading each Bp in solution 4 mL 0.5 mgGEN/mL; taking into account the global coefficient of release at the equilibrium, it is possible to ensure that PSF-GEN can release 2.3 µgGEN and PSB-GEN 1.96 µgGEN. In the rubbery state (T > Tg), the biopolymer chains exhibit increased mobility, thereby enhancing the potential for gentamicin release. This heightened mobility also amplifies the probability of collisions between sulfur–sulfur (S-S) bonds or radical chain ends with components of the bacterial outer membrane or cell wall [24].

The inhibitory effects of the biopolymers against *P. aeruginosa*, a Gram-negative bacterium, were assessed by measuring inhibition zones in agar diffusion tests, as illustrated in Figure 4.

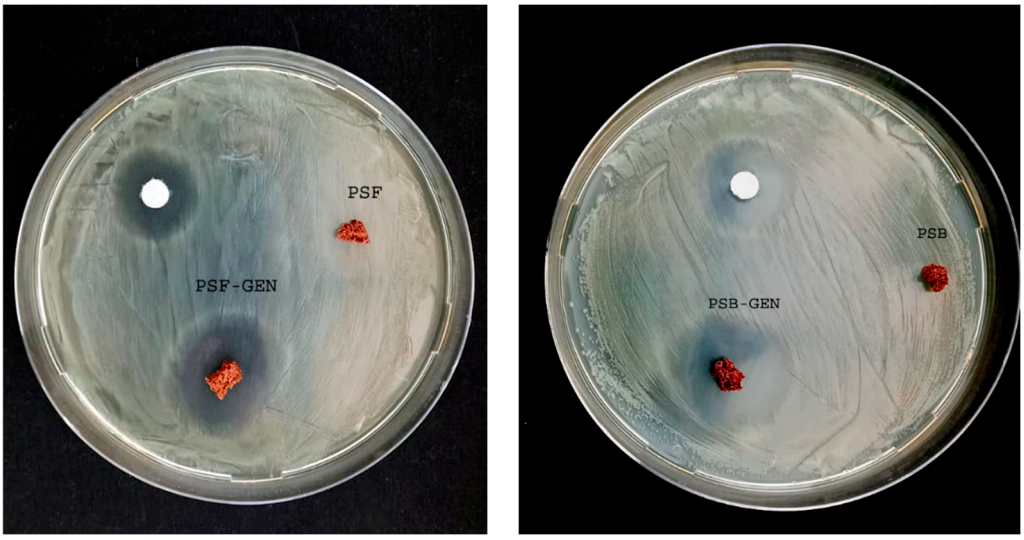

Figure 4. Inhibition halo of GEN, PSF, PSB, PSF-GEN, and PSB-GEN against *P. aeruginosa*.

The diameters of the growth inhibition zones that formed around the different samples after 24 h were measured with a caliper. Our results demonstrate that GEN exhibits inhibitory activity, as evidenced by the presence of an inhibition halo in the positive control. Furthermore, both biopolymers loaded with GEN also displayed antimicrobial activity, as indicated by the appearance of inhibition zones. The inhibitory activity of PSF-GEN and PSB-GEN increased considerably compared with the disc GEN-only. These findings lead us to conclude that the quantity of GEN incorporated by the biopolymers, as well as the amount released, is sufficient to exert an inhibitory effect on the studied strain. Also, the development of an inhibition halo was not visible around both the PSF and PSB biopolymers.

Promising outcomes were observed against *P. aeruginosa*, with the newly developed biocomposites loaded with gentamicin showing significant growth inhibition at 24 h. Importantly, this effect was consistent and did not increase with longer incubation times. The most promising results were obtained when combating *P. aeruginosa*, where the majority of the newly developed biopolymers loaded with gentamicin displayed a significant inhibitory effect on bacterial growth. Table 3 provides a summary of the antibacterial results obtained using the halo method. It is evident that the samples PSF-GEN and PSB-GEN exhibited bacteriostatic activity, while no activity was observed in PSF and PSB against *P. aeruginosa*. Notably, both PSF-GEN and PSB-GEN biocomposites demonstrated the highest levels of antibacterial activity when compared to GEN alone. The enhanced antibacterial activity of PSF-GEN and PSB-GEN compared with the GEN-only may be due to the free length of polysulfide segments. Presently, there are a shortage of published experimental data concerning the impact of sulfur-containing compounds on microorganisms. However, indications suggest that these compounds exert effects on both Gram-positive and Gram-negative bacteria, potentially attributed to the presence of polysulfides [26,37]. There is growing interest in polysulfides as novel antimicrobial agents due to the antimicrobial activity of natural polysulfides found in garlic and onions [37]. Potential reasons for both polymers exhibiting different degrees of antibacterial activity could be due to the degree of cross-linking and the molar ratio of sulfur cross-linkers, and the difference in the GEN loaded inside of the biopolymer.

Table 3. The antibacterial inhibition zones produced by GEN, PSF, PSB, PSF-GEN, and PSB-GEN against *P. aeruginosa*.

Sample Name	Value of Inhibition Halo Diameter [mm]
PSF	0
PSB	0
PSF-GEN	21.10 ± 1.3
PSB-GEN	21.45 ± 1.0
GEN	13.10 ± 1.1

The values are reported in mm as mean ± SD of three replicates.

Antibacterial activity: colony-forming count method. The antibacterial activity of the samples was quantitatively evaluated by the colony-forming unit method against the *P. aeruginosa* strain. As shown in Figure 5, the PSF and PSB biopolymers show an absence of any bactericidal effect. The antibacterial activity results obtained were in accordance with the inhibition halo assay, demonstrating no significant variances between the pristine biopolymers (PSF and PSB) and the control group. However, noteworthy antibacterial efficacy was observed in the PSF-GEN and PSB-GEN biocomposites compared to the control, as evidenced by the presence of inhibition halos. Furthermore, both PSF-GEN and PSB-GEN biocomposites exhibited markedly heightened antibacterial potency against bacterial strains compared to the GEN-only, achieving a reduction in the number of colonies (CFU/mL) more than 2 log10. Remarkably, PSB-GEN showcased superior inhibition activity displaying a twofold reduction in comparison to the control and the pristine biopolymers, as evidenced by the inhibition in halo size.

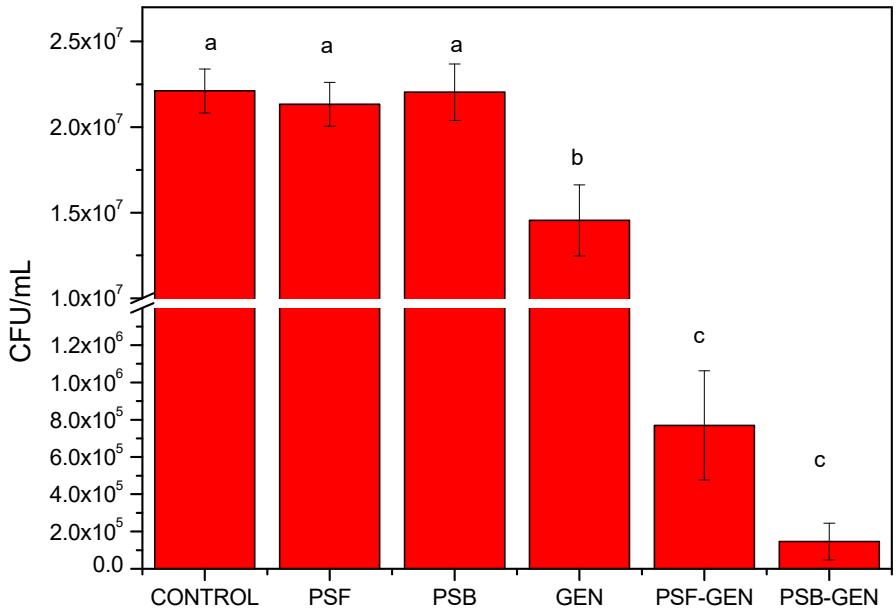

Figure 5. Cell Viability of *P. aeruginosa* of different treatments. Values represent mean ± SE. Different letters indicate significant statistical differences between treatments $p < 0.01$.

4. Conclusions

In conclusion, this study presents the synthesis of solid cross-linked biopolymers derived from soybean (PSB) and sunflower (PSF) oils through an environmentally friendly process involving inverse vulcanization with sulfur. The biopolymers were characterized using several techniques that allow ensuring the formation of 3D structures by cross-linking the unsaturation of the oils with sulfur. These biopolymers effectively incorporated the antibiotic gentamicin (GEN), resulting in the development of novel biocomposite materials.

Notably, both PSF and PSB biopolymers exhibited greater swelling in the GEN solution compared to pure water, indicating effective sorption of the hydrophobic antibiotic onto the hydrophobic biopolymer matrices. Furthermore, successful release of GEN from the biocomposites was demonstrated, leading to inhibition of *P. aeruginosa* growth, as evidenced by inhibition halo assays. Remarkably, PSB-GEN and PSF-GEN biocomposites exhibited potent antibacterial activity against the Gram-negative pathogen *P. aeruginosa*. Of particular interest is the observation that both biocomposites exhibited markedly enhanced antibacterial efficacy compared to a control consisting of GEN-loaded filter paper. This suggests that the retention and release of GEN within the biopolymer matrices are more pronounced, likely due to the hydrophobic nature of both GEN and the biopolymers.

Overall, these findings underscore the potential of these biocomposites as promising candidates for combating bacterial infections, highlighting their ability to effectively load, retain, and release antimicrobial agents, thus offering a sustainable and eco-friendly approach to developing antimicrobial materials.

Author Contributions: The experimental work and initial writing were completed by E.I.Y. and D.F.A. Research concept, interpretation of results, and editing of the manuscript were through contributions of all authors. All authors have read and agreed to the published version of the manuscript.

Funding: This research was funded by FONCYT (PICT 00099/2021 and PICT 00066/2021), CONICET (PIP 11220210100323CO) and SECYT-UNRC (PPI-C616-2 and PPI- B263-1).

Institutional Review Board Statement: Not applicable.

Informed Consent Statement: Not applicable.

Data Availability Statement: The data that support the findings of this study are available from the corresponding author upon reasonable request.

Acknowledgments: E.I. Yslas, M.V. Martinez, C. Barbero, and D.F. Acevedo are permanent research fellows of CONICET; A.S. Farioli thanks CONICET for postgraduate research fellowships.

Conflicts of Interest: The authors declare no conflict of interest. The funders had no role in the design of this study; in the collection, analyses or interpretation of data; in the writing of the manuscript; or in the decision to publish the results.

References

1. Wang, H.; Zhao, B.; Dong, W.; Zhong, Y.; Zhang, X.; Gong, Y.; Zhan, R.; Xing, M.; Zhang, J.; Luo, G.; et al. A dual-targeted platform based on graphene for synergistic chemo-photothermal therapy against multidrug-resistant Gram-negative bacteria and their biofilms. *Chem. Eng. J.* **2020**, *393*, 124595. [CrossRef]
2. Mirabal-Álvarez, G.A. Resistencia a los antimicrobianos en hospitales infantiles: Perspectiva y realidad. *Rev. Biomédica* **2020**, *31*, 1–2. [CrossRef]
3. Roope, L.S.J.; Smith, R.D.; Pouwels, K.B.; Buchanan, J.; Abel, L.; Eibich, P.; Butler, C.C.; Tan, P.S.; Sarah Walker, A.; Robotham, J.V.; et al. The challenge of antimicrobial resistance: What economics can contribute. *Science* **2019**, *364*, eaau4679. [CrossRef]
4. Pons, M.J.; Ruiz, J. Current trends in epidemiology and antimicrobial resistance in intensive care units. *J. Emerg. Crit. Care Med.* **2019**, *3*, 5. [CrossRef]
5. De Oliveira, D.M.P.; Forde, B.M.; Kidd, T.J.; Harris, P.N.A.; Schembri, M.A.; Beatson, S.A.; Paterson, D.L.; Walker, M.J. Antimicrobial resistance in ESKAPE pathogens. *Clin. Microbiol. Rev.* **2020**, *33*, 10-1128. [CrossRef]
6. Tacconelli, E.; Carrara, E.; Savoldi, A.; Harbarth, S.; Mendelson, M.; Monnet, D.L.; Pulcini, C.; Kahlmeter, G.; Kluytmans, J.; Carmeli, Y.; et al. Discovery, research, and development of new antibiotics: The WHO priority list of antibiotic-resistant bacteria and tuberculosis. *Lancet Infect. Dis.* **2018**, *18*, 318–327. [CrossRef]
7. Pokharel, K.; Dawadi, B.R.; Bhatt, C.P.; Gupte, S. Prevalence of Pseudomonas Aeruginosa and its Antibiotic Sensitivity Pattern. *J. Nepal Health Res. Counc.* **2019**, *17*, 109–113. [CrossRef]
8. Peix, A.; Ramírez-Bahena, M.H.; Velázquez, E. Historical evolution and current status of the taxonomy of genus Pseudomonas. *Infect. Genet. Evol.* **2009**, *9*, 1132–1147. [CrossRef]
9. Mancuso, G.; Midiri, A.; Gerace, E.; Biondo, C. Bacterial Antibiotic Resistance: The Most Critical Pathogens. *Pathogens* **2021**, *10*, 1310. [CrossRef]
10. Barber, M.; Waterworth, P.M. Activity of Gentamicin Against Pseudomonas and Hospital Staphylococci. *Br. Med. J.* **1966**, *1*, 203–205. [CrossRef]

11. Verma, D.; Yadav, A.K.; Solanki, P.R. Nanocomposites applications in wound management. In *Nanotechnological Aspects for Next-Generation Wound Management*; Academic Press: Cambridge, MA, USA, 2024; pp. 149–167. [CrossRef]
12. Liu, J.; Wu, M.; Lu, J.; He, Q.; Zhang, J. Janus Intelligent Antibacterial Hydrogel Dressings for Chronic Wound Healing in Diabetes. *ACS Appl. Polym. Mater.* **2023**, *5*, 2596–2606. [CrossRef]
13. Kondaveeti, S.; de Assis Bueno, P.V.; Carmona-Ribeiro, A.M.; Esposito, F.; Lincopan, N.; Sierakowski, M.R.; Petri, D.F.S. Microbicidal gentamicin-alginate hydrogels. *Carbohydr. Polym.* **2018**, *186*, 159–167. [CrossRef]
14. Cheng, C.H.; Chen, Y.S.; Chang, H.T.; Chang, K.C.; Huang, S.M.; Liu, S.M.; Chen, W.C. In vitro evaluation of antibacterial activity and biocompatibility of synergistically cross-linked gelatin-alginate hydrogel beads as gentamicin carriers. *J. Drug Deliv. Sci. Technol.* **2023**, *79*, 104078. [CrossRef]
15. Divyashri, G.; Badhe, R.V.; Sadanandan, B.; Vijayalakshmi, V.; Kumari, M.; Ashrit, P.; Bijukumar, D.; Mathew, M.T.; Shetty, K.; Raghu, A.V. Applications of hydrogel-based delivery systems in wound care and treatment: An up-to-date review. *Polym. Adv. Technol.* **2022**, *33*, 2025–2043. [CrossRef]
16. Chung, W.J.; Griebel, J.J.; Kim, E.T.; Yoon, H.; Simmonds, A.G.; Ji, H.J.; Dirlam, P.T.; Glass, R.S.; Wie, J.J.; Nguyen, N.A.; et al. The use of elemental sulfur as an alternative feedstock for polymeric materials. *Nat. Chem.* **2013**, *5*, 518–524. [CrossRef]
17. Farioli, A.S.; Martinez, M.V.; Barbero, C.; Yslas, E.; Acevedo, D. The effect of oil raw material composition in the synthesis of bio-sorbents based on inverse vulcanization on the ability to remediate hydrocarbon-contaminated water. A novel method for decontaminating water/fuel emulsions. *J. Appl. Polym. Sci.* **2023**, *141*, e54914. [CrossRef]
18. Abbasi, A.; Yahya, W.Z.N.; Nasef, M.M. Sulfur-based polymers by inverse vulcanization: A novel path to foster green chemistry. *Green Mater.* **2020**, *8*, 172–180. [CrossRef]
19. Chalker, J.M.; Mann, M.; Worthington, M.J.H.; Esdaile, L.J. Polymers Made by Inverse Vulcanization for Use as Mercury Sorbents. *Org. Mater.* **2021**, *3*, 362–373. [CrossRef]
20. Nayeem, A.; Ali, M.F.; Shariffuddin, J.H. Recovery of waste cooking palm oil as a crosslinker for inverse vulcanized adsorbent to remove iron (Fe3+) ions. *J. Environ. Chem. Eng.* **2024**, *12*, 111853. [CrossRef]
21. Ghumman, A.S.M.; Shamsuddin, R.; Abbasi, A.; Ahmad, M.; Yoshida, Y.; Sami, A.; Almohamadi, H. The predictive machine learning model of a hydrated inverse vulcanized copolymer for effective mercury sequestration from wastewater. *Sci. Total Environ.* **2024**, *908*, 168034. [CrossRef]
22. Mann, M.; Kruger, J.E.; Andari, F.; McErlean, J.; Gascooke, J.R.; Smith, J.A.; Worthington, M.J.H.; McKinley, C.C.C.; Campbell, J.A.; Lewis, D.A.; et al. Sulfur polymer composites as controlled-release fertilisers. *Org. Biomol. Chem.* **2019**, *17*, 1929–1936. [CrossRef] [PubMed]
23. Miao, C.; Xun, X.; Dodd, L.J.; Niu, S.; Wang, H.; Yan, P.; Wang, X.C.; Li, J.; Wu, X.; Hasell, T.; et al. Inverse Vulcanization with SiO_2-Embedded Elemental Sulfur for Superhydrophobic, Anticorrosion, and Antibacterial Coatings. *ACS Appl. Polym. Mater.* **2022**, *4*, 4901–4911. [CrossRef]
24. Dop, R.A.; Neill, D.R.; Hasell, T. Antibacterial Activity of Inverse Vulcanized Polymers. *Biomacromolecules* **2021**, *22*, 5223–5233. [CrossRef] [PubMed]
25. Dop, R.A.; Neill, D.R.; Hasell, T. Sulfur-Polymer Nanoparticles: Preparation and Antibacterial Activity. *ACS Appl. Mater. Interfaces* **2023**, *15*, 20822–20832. [CrossRef]
26. Smith, J.A.; Mulhall, R.; Goodman, S.; Fleming, G.; Allison, H.; Raval, R.; Hasell, T. Investigating the Antibacterial Properties of Inverse Vulcanized Sulfur Polymers. *ACS Omega* **2020**, *5*, 5229–5234. [CrossRef]
27. Pereyra, J.Y.D.C.; Barbero, C.A.; Acevedo, D.; Yslas, E. Antibacterial effects of in-situ zinc oxide nanoparticles generated inside the poly (acrylamide-co-hydroxyethylmethacrylate) nanocomposite. *Nanotechnology* **2022**, *34*, 045101. [CrossRef]
28. Wu, X.; Smith, J.A.; Petcher, S.; Zhang, B.; Parker, D.J.; Griffin, J.M.; Hasell, T. Catalytic inverse vulcanization. *Nat. Commun.* **2019**, *10*, 647. [CrossRef]
29. Zhang, Y.; Glass, R.S.; Char, K.; Pyun, J. Recent advances in the polymerization of elemental sulphur, inverse vulcanization and methods to obtain functional Chalcogenide Hybrid Inorganic/Organic Polymers (CHIPs). *Polym. Chem.* **2019**, *10*, 4078–4105. [CrossRef]
30. Bushuev, Y.G.; Grosu, Y.; Chorążewski, M.A.; Meloni, S. Effect of the Topology on Wetting and Drying of Hydrophobic Porous Materials. *ACS Appl. Mater. Interfaces* **2022**, *14*, 30067–30079. [CrossRef] [PubMed]
31. Ganji, F.; Vasheghani-Farahani, S.; Vasheghani-Farahani, E. Theoretical description of hydrogel swelling: A review. *Iran. Polym. J.* **2010**, *19*, 375–398.
32. Ismail, O.; Kipcak, A.S.; Piskin, S. Modeling of absorption kinetics of poly(acrylamide) hydrogels crosslinked by EGDMA and PEGDMAs. *Res. Chem. Intermed.* **2013**, *39*, 907–919. [CrossRef]
33. Üzüm, Ö.B.; Karadağ, E. Equilibrium swelling studies of chemically cross-linked highly swollen acrylamide-sodium acrylate hydrogels in various water-solvent mixtures. *Polym. Plast. Technol. Eng.* **2010**, *49*, 609–616. [CrossRef]
34. Barbero, C.A.; Martínez, M.V.; Acevedo, D.F.; Molina, M.A.; Rivarola, C.R. Cross-Linked Polymeric Gels and Nanocomposites: New Materials and Phenomena Enabling Technological Applications. *Macromol* **2022**, *2*, 440–475. [CrossRef]
35. Azizian, S. Kinetic models of sorption: A theoretical analysis. *J. Colloid Interface Sci.* **2004**, *276*, 47–52. [CrossRef] [PubMed]

36. Martínez, M.V.; Rivarola, C.R.; Miras, M.C.; Barbero, C.A. A colorimetric iron sensor based on the partition of phenanthroline complexes into polymeric hydrogels. Combinatorial synthesis and high throughput screening of the hydrogel matrix. *Sens. Actuators B Chem.* **2017**, *241*, 19–32. [CrossRef]
37. Tsao, S.M.; Yin, M.C. In vitro activity of garlic oil and four diallyl sulphides against antibiotic-resistant Pseudomonas aeruginosa and Klebsiella pneumoniae. *J. Antimicrob. Chemother.* **2001**, *47*, 665–670. [CrossRef]